

# 19th century glacier representations and fluctuations in the central and western European Alps: An interdisciplinary approach

H.J. Zumbühl\*, D. Steiner\*, S.U. Nussbaumer

*Institute of Geography, University of Bern, Hallerstrasse 12, CH-3012 Bern, Switzerland*

Received in revised form 22 August 2006; accepted 24 August 2006

Available online 22 February 2007

## Abstract

European Alpine glaciers are sensitive indicators of past climate and are thus valuable sources of climate history. Unfortunately, direct determinations of glacier changes (length variations and mass changes) did not start with increasing accuracy until just before the end of the 19th century. Therefore, historical and physical methods have to be used to reconstruct glacier variability for preceding time periods.

The Lower Grindelwald Glacier, Switzerland, and the Mer de Glace, France, are examples of well-documented Alpine glaciers with a wealth of different historical sources (e.g. drawings, paintings, prints, photographs, maps) that allow reconstruction of glacier length variations for the last 400–500 years. In this paper, we compare the length fluctuations of both glaciers for the 19th century until the present.

During the 19th century a majority of Alpine glaciers – including the Lower Grindelwald Glacier and the Mer de Glace – have been affected by impressive glacier advances. The first maximum extent around 1820 has been documented by drawings from the artist Samuel Birmann, and the second maximum extent around 1855 is shown by photographs of the Bisson Brothers. These pictorial sources are among the best documents of the two glaciers for the 19th century.

In addition to an analysis of historical sources of the 19th century, we also study the sensitivity of the Lower Grindelwald Glacier to climate parameters (multiproxy reconstructions of seasonal temperature and precipitation) for an advance and a retreat period in the 19th century using a new neural network approach. The advance towards 1820 was presumably driven by low summer temperatures and high autumn precipitation. The 1860–1880 retreat period was mainly forced by high temperatures. Finally, this nonlinear statistical approach is a new contribution to the various investigations of the complex climate–glacier system.

© 2007 Elsevier B.V. All rights reserved.

*Keywords:* glacier fluctuations; historical sources; sensitivity analysis; neural network

## 1. Introduction

During the 19th century impressive glacier advances affected the majority of the Alpine glaciers. This can be

deduced from natural archives and a wealth of documentary evidence (e.g. Zumbühl and Holzhauser, 1988; Maisch et al., 1999). In general, historical records give a detailed picture of glacial fluctuations and allow studying glacier history further back in time than would be possible from direct measurements alone (e.g. Holzhauser et al., 2005). For instance, empirical qualitative and/or quantitative data on the length, area and volume of glaciers can be derived from these sources.

\* Corresponding authors. Tel.: +41 31 631 85 51; fax: +41 31 631 85 11.

E-mail addresses: [zumbuehl@giub.unibe.ch](mailto:zumbuehl@giub.unibe.ch) (H.J. Zumbühl), [steiner@giub.unibe.ch](mailto:steiner@giub.unibe.ch) (D. Steiner).

This study focuses on two well-documented Alpine glaciers, the Lower Grindelwald Glacier, Switzerland, and the Mer de Glace, France (Fig. 1). For both glaciers

we present different kinds of historical pictorial sources (drawings and photographs) that together document the 19th century glacier maximum extents around 1820

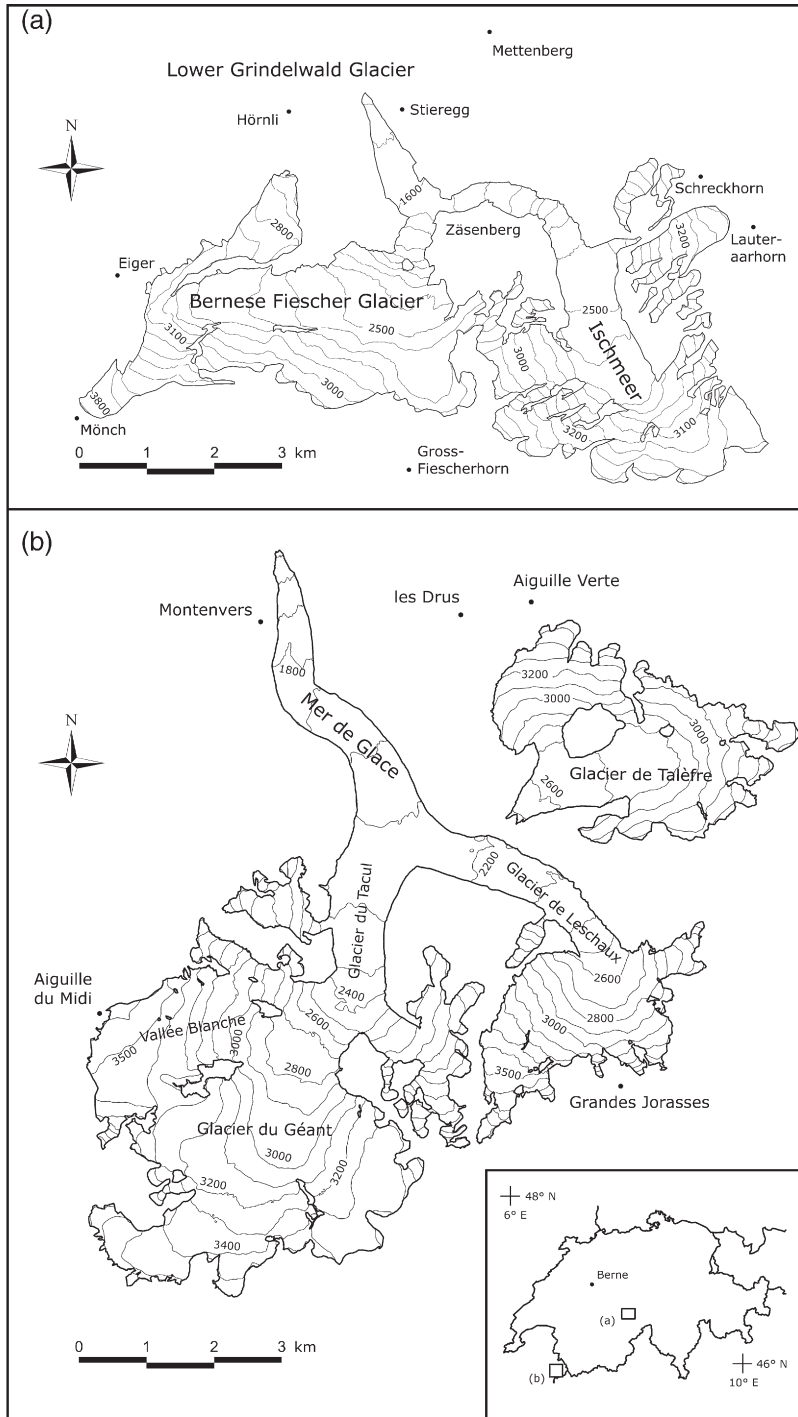


Fig. 1. Geographical location of study sites: (a) the Grindelwald region with the Lower Grindelwald Glacier, (b) the Mont Blanc region with the Mer de Glace.

and 1855. Samuel Birmann (1793–1847), an important Swiss landscape artist, portrayed the Lower Grindelwald Glacier and the Mer de Glace at their first maximum extent around 1820 in detailed drawings of their glacier snouts. The Bisson Brothers, famous photographers of that time, made pictures of the two glaciers at their second maximum extent around 1855, again including detailed views of their glacier snouts. Therefore, the historical sources of the two glaciers allow comparison of these extraordinary high-quality glacier representations at their maximum extent. It must be noted that the change of glacier representation techniques from drawings to photographs demonstrates also the changing view on glaciers from the magic to the scientific (Haerberli and Zumbühl, 2003; Steiner et al., in press).

Furthermore, the 19th century provides also an opportunity to analyze the climatic conditions of the last widespread glacier advance and the following retreat. This is done by connecting new gridded reconstructions of temperature and precipitation (Luterbacher et al., 2004; Pauling et al., 2006) with the data of length fluctuations of the Lower Grindelwald Glacier. Because the climate–glacier relation is, in part, nonlinear (Steiner et al., 2005), we suggest a new statistical nonlinear approach based on a neural network to investigate the climate–glacier system, i.e. to study the meteorological conditions which led to a glacier advance or retreat. In a sensitivity analysis that explores the significance of climatic inputs to the glacier system we evaluate the relevant climatic variables that caused the advance towards 1820 and the rapid retreat of the Lower Grindelwald Glacier after 1860.

In this paper, we compare the length fluctuations of the Lower Grindelwald Glacier and the Mer de Glace since 1800. Since this approach is descriptive, we also present a neural network model to explore potential climate forcings to explain glacier length fluctuations with the Lower Grindelwald Glacier. Therefore, the analysis of historical sources provides a framework for which we can test the relative importance of climate variables forcing glacier advance and retreat.

## 2. Data and methods

### 2.1. Study area

Our study focuses on the Lower Grindelwald Glacier, located in the northern Bernese Alps (Switzerland), and the Mer de Glace, located on the north face

of the Mont Blanc (France). The topography and some landmark locations of these two glaciers are shown in Fig. 1.

The Lower Grindelwald Glacier (46°35' N, 8°05' E) is a valley glacier, 8.85 km long and covering a surface of 20.6 km<sup>2</sup>. Ischmeer in the east and the Bernese Fiescher Glacier in the west join to form the tongue of the Lower Grindelwald Glacier (Fig. 1a). The main contribution of ice presently originates from the Bernese Fiescher Glacier (Holzhauser and Zumbühl, 1996; Schmeits and Oerlemans, 1997). The approximated equilibrium line altitude (ELA), derived from digital elevation models (DEMs), is at 2640 m a.s.l. The glacier today terminates at 1297 m a.s.l. in a narrow gorge so that reliable observations are difficult to obtain (data from 2004: Steiner et al., in press).

The Mer de Glace (45°54' N, 8°57' E) *sensu lato* is a compound valley glacier, 12.0 km long and covering a surface of 31.9 km<sup>2</sup> (without including Glacier de Talèfre). The glacier is fed by several tributaries with the Glacier du Géant being the most important one (Fig. 1b). Since the 1931–1969 retreat, the Glacier du Talèfre is separated from the main ice stream. The Mer de Glace *sensu stricto* refers to the lowest approximately 5 km of the ice stream, forming the glacier tongue beneath Montenvers. The ELA is situated at around 2775 m a.s.l., and the glacier today terminates at 1467 m a.s.l. (data from 2001: Nussbaumer et al., in press).

The Bernese Alps is a group of mountain ranges in the central part of the Alps drained by the river Aare and its tributary Saane in the north, and the Rhône in the south and the Reuss in the east. The northern part of the Bernese Alps, including the Lower Grindelwald Glacier, is exposed to the westerlies and receives maximum precipitation during summer, with low variability. The mean annual temperature at Grindelwald (1040 m a.s.l.), located approximately 3 km from the glacier front of the Lower Grindelwald Glacier, was 6.7 °C during the 1966–1989 period. The mean temperature during the accumulation season (October–April) and ablation season (May–September) during the 1966–1989 period was 2.3 °C and 12.9 °C, respectively.

The mean annual precipitation during the 1961–1990 period was 1428 mm with precipitation during the accumulation season (October–April) and ablation season (May–September) of 720 mm and 708 mm, respectively (data from the online database of Meteo-Swiss). Because of high precipitation (locally exceeding 4000 mm per year), the Bernese Alps have a relative low glacier equilibrium line altitude and is the heaviest glacierized region in the Alps. Both the glacier with the lowest front (Lower Grindelwald Glacier) and the

largest glacier of the Alps (Great Aletsch Glacier) are located within this region (Kirchhofer and Sevruc, 1992; Imhof, 1998).

Due to the extraordinary low position of the terminus and its easy accessibility, the Lower Grindelwald Glacier is one of the best-documented glaciers in the Swiss Alps, and likely in the world. The cumulative length fluctuations of the Lower Grindelwald Glacier, derived from documentary evidence, covers the period 1535–1983 including the two well-known glacier maxima about 1600 and 1855/56 (Zumbühl, 1980; Holzhauser and Zumbühl, 1996, 2003).

The Mont Blanc mountain range (Fig. 1) extends 50 km from Martigny (Switzerland) in the northeast to St. Gervais (France) in the southwest, forming the watershed between France and Italy and separating the uppermost catchment areas of the Rhône and Po rivers. On the French side of the mountain range, the upper Arve river flows down the deep trough of Chamonix, with several glaciers (Glacier du Tour, Glacier d'Argentière, Mer de Glace, Glacier des Bossons) draining into this river. Climate in the valley of Chamonix is typical for the western Alps and comparable to the Grindelwald area, although slightly drier. Annual temperature of the Chamonix meteorological station (1054 m a.s.l.) is 6.6 °C for the 1935–1960 period, the annual precipitation amounts to 1262 mm for the 1934–1962 period (Wetter, 1987).

The Mer de Glace is the longest and largest glacier of the western Alps. During the Little Ice Age (LIA), the period lasting a few centuries between the Middle Ages and the warming of the first half of the 20th century (Grove, 2004), the glacier nearly continuously reached the bottom of the valley of Chamonix at 1000 m a.s.l. This lowest part of Mer de Glace was called Glacier des Bois which today has completely melted away. Similar to the Lower Grindelwald Glacier, the Mer de Glace has been well observed by scientists, artists, and travellers since the beginning of alpinism, leading to a large number of historical documentary data.

## 2.2. Historical sources in glaciology

If sufficient in quality and quantity, written documents and pictorial historical records (paintings, sketches, engravings, photographs, chronicles, topographic maps, reliefs) provide a detailed picture of glacier fluctuations over the last few centuries. Using these data, we can achieve a resolution of decades or, in some cases, even individual years of ice margin positions (Zumbühl and Holzhauser, 1988; Holzhauser

et al., 2005). The density of historical material prior to 1800 highly depends on the elevation of the tongue and the relationship between settlements and cultivated land and the glacier advances.

Historical data have to be considered carefully and local circumstances need to be taken into account. The evaluation of historical sources, the so-called historical method, has to fulfill some conditions in order to obtain reliable results concerning former glacier extents (Zumbühl and Holzhauser, 1988): Firstly, the dating of the document has to be known or reconstructed. This often includes labour-intensive archive work. Secondly, the glacier and its surroundings have to be represented realistically and topographically correct which requires certain skills of the corresponding artist. In addition, the artist's topographic position should be known; prominent features in the glacier's surroundings such as rock steps, hills or mountain peaks facilitate the evaluation of historical documentary data.

Note that for both the Lower Grindelwald Glacier, and the Mer de Glace, there is a wealth of historical (pictorial) documents which has been evaluated. Probably the best example of a glacier curve derived from historical sources is the series of cumulative length changes of the Lower Grindelwald Glacier (Zumbühl, 1980; Zumbühl et al., 1983).

## 2.3. Sensitivity analysis by neural networks

The evaluation of historical data gives insight into the change in glacier length over time without showing the climatic driving factors which presumably affected these glacier changes. To investigate the relationship between the meteorological conditions and variations of glaciers many studies have been carried out. For instance, regression techniques with different numbers and types of predictors have often been used (Oerlemans and Reichert, 2000, and references therein). Besides these classical methods that commonly use linear assumptions, neural network models (NNMs) have become popular for performing nonlinear regression and classification (Steiner et al., 2005, and references therein). Because glacier length is a complex function dependent on climate, time, glacier geometry and other factors, it may be well-suited to nonlinear model approaches. Therefore, modelling results can complement the historical analysis in order to give a better picture of how, and why the glacier has reacted.

Inspired by the human brain, a neural network (NN) consists of a set of highly interconnected units, which

process information as a response to external stimuli. A neural network is thus a simplistic mathematical representation of the brain that emulates the signal integration and threshold firing behaviour of biological neurons by means of mathematical equations.

The most widely used NN models are the feed-forward neural networks (Rumelhart et al., 1986). Their applications cover a broad field of the environmental sciences including meteorology and climatology. Some examples of recent applications using NN include the detection of anthropogenic climate change (Walter and Schönwiese, 2002, 2003) and the study of an Alpine glacier mass balance (Steiner et al., 2005).

In this study the standard NN model, the Back-propagation Network (BPN), was applied (Rumelhart et al., 1986). This network architecture is based on a supervised learning algorithm to find a minimum cost function. Because this approach bears a certain risk of overfitting, the data have to be separated into a training and a validation subset. The actual ‘learning’ process of the network is performed on the training subset only, whereas the validation subset serves as an independent reference for the simulation quality. This technique is called Cross-Validation (Stone, 1974; Michaelsen, 1987). When applying NN models to a nonstationary time series, as in this approach, the training subset includes the full range of extremes in both predictors and predictands. Otherwise, the algorithm will fail during the validation process if confronted with an extreme value that was not part of the training subset. We used 75% of all data for training

and the remaining 25% for validation (Walter and Schönwiese, 2003).

A typical NN model consists of three layers: input, processing and output layers (Fig. 2). The input to an NN model is a vector of elements  $x_k$ , where the index  $k$  stands for the number of input units in the network. In this study two new gridded ( $0.5^\circ \times 0.5^\circ$  resolution) multiproxy reconstructions of seasonal temperature (Luterbacher et al., 2004) and precipitation fields (Pauling et al., 2006) from 1500–2000 for European land areas were used as input data. These inputs serve as climatic driving factors to the glacier system. Before processed the inputs are weighted with weights  $w_{jk}$  where  $j$  represents the number of processing units, to give the inputs to the processing units.

Using too few/many processing units can lead to underfitting/overfitting problems because the simulation results are highly sensitive to the number of processing units and learning parameters. Therefore a variety of BPNs must be checked to obtain robust results.

For the simulation of the glacier length variations of the Lower Grindelwald Glacier we used six potential input units as forcings (Temp\_MAM, Temp\_JJA, Temp\_SON, Prec\_DJF, Prec\_MAM, Prec\_SON), each of them have been stepwise shifted so that all lags between 0 and 45 years are considered to account for the uncertain and changing reaction time of this glacier. As target function we apply the curve of length variations of the Lower Grindelwald Glacier. In this manner the NN model will use those shifted input series that explain the glacier length variations. Hence, there are  $46 \cdot 6 = 276$  input units (climate variables), 138 processing units in 1

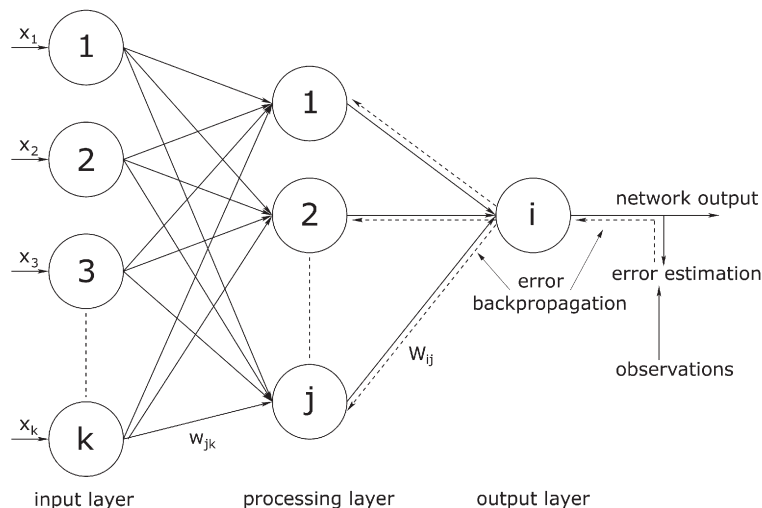


Fig. 2. An example of a simplified 3-layer k-j-1 BPN architecture. The concept of the backpropagation training algorithm is shown by several arrows (from Steiner et al., 2005). Note that in our study the input layer consists of the climatic inputs and the output layer represents the glacier length.



processing layer and the length fluctuations as output unit. This neural network architecture is abbreviated as 276-138-1.

After weighting and adding of the inputs, the results were passed to nonlinear activation functions (e.g. sigmoid functions) in each processing unit (processing layer in Fig. 2). These functions produced the output of the processing layer. The outputs of the processing units are fed to the output layer where they are again weighted with the weights  $W_{ij}$ . The use of a second activation function will finally produce the output of the network (output layer in Fig. 2).

The purpose of training an NN model is to find a set of coefficients that reduces the error between the model outputs and the given test data  $y(x_k)$ . This is usually done by adjusting the weights  $W_{ij}$  and  $w_{jk}$  to minimize the least square error. One way to adjust these weights is error backpropagation. The backpropagation training consists of two passes of computation: a forward pass and a backward pass. In the forward pass an input vector is applied to the units in the input layer. The signals from the input layer propagate to the units in the processing layer and each unit produces an output. The outputs of these units are propagated to units in subsequent layers. This process continues until the signals reach the output layer where the actual response of the network to the input vector is obtained. During the forward pass the weights of the network are fixed. During the backward pass (see dashed arrows in Fig. 2), on the other hand, the weights are all adjusted in accordance with an error signal that is propagated backward through the network against the initial direction.

As mentioned above, this network architecture still bears the risk of being stuck in local minima on the error hypersurface. To reduce this risk, conjugate gradient descent was used in this study. This is an improved version of standard backpropagation with accelerated convergence. A detailed description of this technique can be found in Steiner et al. (2005).

A second uncertainty in the BPN simulation is related to the fact that the identified minimum is dependent on the starting point on the error hypersurface. To reduce this kind of uncertainty, the BPN was performed 30 times, each time only varying the starting point on the error hypersurface. Finally, the average of the 30 model results has been analyzed.

Sensitivity analysis using neural networks is based on the measurements of the effect that is observed in the output layer due to changes in the input data. A common way to perform this analysis consists of comparing the error made by the network from the original patterns

with the error made when restricting the input of interest to the average value. Thus, the greater the increase in the error function upon restricting the input, the greater the importance of this input in the output (e.g. Wang et al., 2000). In this study we kept one seasonal temperature or precipitation input constant while the other inputs were allowed to fluctuate. The observed error of glacier response gave us indications of its sensitivity to the input that was constant.

### 3. Results

#### 3.1. *Two glaciers drawn by the artist Samuel Birmann — The first advance in the 19th century*

On the pencil watercolor drawing by Samuel Birmann (1793–1847) made in September 1826 (Fig. 3a), the marked fanshaped tongue – the “Schweif” or tail (covering the Schopfrocks) – of the Lower Grindelwald Glacier extends far down into the valley. The skyline of the drawing is dominated by the Mettenberg (left), the Fiescherhorn (center background) and the Hörnligrat (right; see Fig. 1). In the foreground of the glacier (right) we can clearly recognize a complex moraine system. The wooden area between the ice front and the moraine walls shows that the Lower Grindelwald Glacier reached a bigger extension in earlier times (around 1600; Zumbühl, 1980), and that the 1814–1820/22 advance amounts to 450–520 m, approximately 75–150 m behind the greatest LIA extension around 1600.

In this context it must be noted that Samuel Birmann from Basel was “the most important Swiss romantic of topographic landscape artists” (Zumbühl, 1997). We know of approximately 100 views of glaciers, all produced within 20 years (1815–1835). The drawings are all of an outstanding topographic quality and due to the very wide angle often used in his views, they are comparable to photographs, in many ways even superior to them.

Among this unique collection of glacier views by Samuel Birmann, there is also a pencil watercolor drawing of the Mer de Glace from 1823 (Fig. 3b). The drawing shows the impressive peaks of the Aiguille Verte and les Drus (skyline) and the ice flow of the Glacier des Bois that terminated near the village of les Bois (roof and chimneys with smoke) in the valley bottom. Similar to Grindelwald with the Schopfrocks the ice front terminates in a rocky zone, Rochers des Mottets (middleground between village and peaks). A close look reveals also the moraines of Côte du Piget (left).



Fig. 3. The Swiss artist Samuel Birmann (1793–1847) portrayed (a) the Lower Grindelwald Glacier in September 1826 (39.2 × 49.7 cm; pencil, pen, watercolor, bodycolor), (b) the Mer de Glace in August 1823 (44.3 × 58.9 cm; pencil, pen, watercolor, bodycolor). Kupferstichkabinett, Kunstmuseum Basel. Photographs by Heinz J. Zumbühl.

In the “Souvenirs de la vallée de Chamonix”, a precious artbook with aquatints (colorprints), Samuel Birmann writes to view No. 21 “Glacier des Bois”: “In 1821, the glacier advanced until twenty feet to a house of the village [les Bois]; so the people prepared to leave their homes, but this time, the glacier respected his limits, and since then he started to melt back slowly” (translated from Birmann, 1826). The advance, starting around 1800 and ending in 1821, pushed the ice front in

the valley approximately 560 m (Nussbaumer et al., in press). This amount is similar to Grindelwald, but the advance took place in a shorter time. In 1821, the Mer de Glace reached the largest extension in the 19th century, comparable to the Rosenlauri Glacier in 1826 (Zumbühl and Holzhauser, 1988), but different to the Lower Grindelwald Glacier which reached its peak in 1855/56.

The same artist offers us also detailed views of the fronts of the glaciers mentioned with two huge glacier



snouts in the valley bottom. Firstly, the Mer de Glace in 1823 with the source of the l'Arveyron is shown in Fig. 4b, and secondly, the Lower Grindelwald Glacier in 1826 with the source of the Lütschine is shown in Fig. 4a.

### 3.2. Two glaciers from the same photographer family (the Bisson Brothers) — The second mid 19th century advance

The mid 19th century was in many ways a very interesting time. Firstly, it brought the second advance and for many glaciers the maximum extension in the 19th century. Secondly, this time brought also a revolutionary change of glacier representation techni-

ques, from drawings and prints to the much more precise first photographs.

The probably first photograph of the Lower Grindelwald Glacier was taken by the Bisson Brothers (Fig. 5a). Louis Auguste Bisson “the older” (1814–1876), originally architect, and his brother Auguste Rosalie Bisson, “the younger” (1826–1900), originally painter, founded in 1840 a company for producing daguerreotypes. Later, they became very famous for their impressive photographic views of the Mont Blanc. These views were made for the French emperor Napoléon III.

One of the big challenges using historical pictorial views in glacier reconstructions is the precise dating of the data sources, especially for photographs. Thanks to

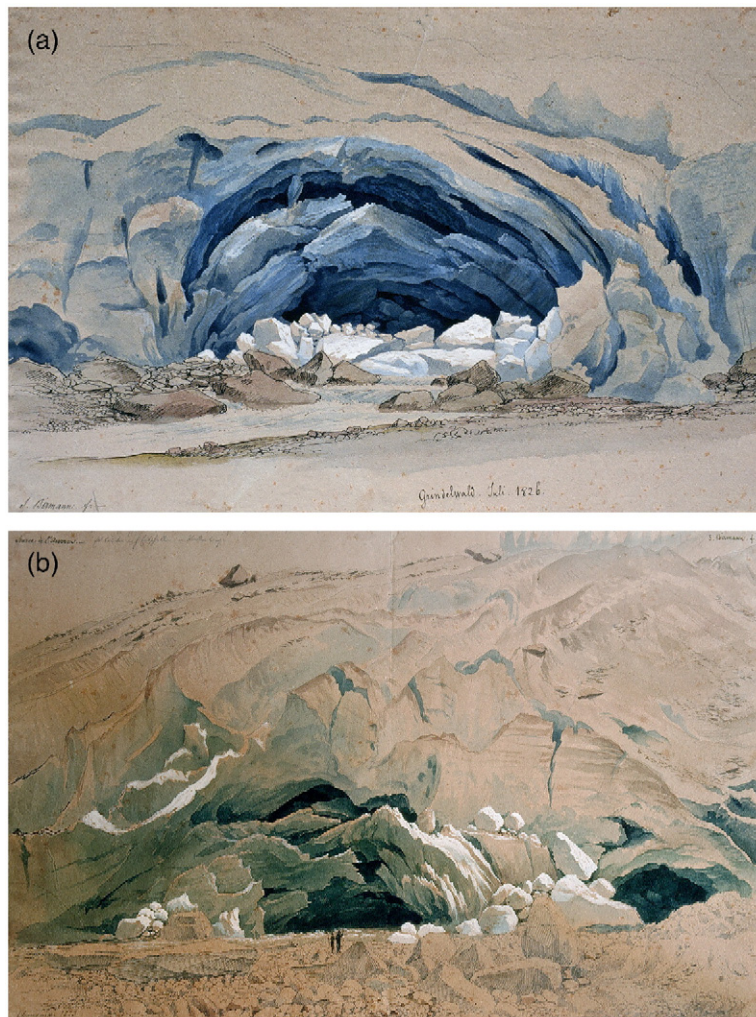


Fig. 4. Samuel Birmann also produced detailed views of the glacier snouts of (a) the Lower Grindelwald Glacier in July 1826 (30.3 × 45.2 cm; pencil, pen, watercolor, bodycolor) and (b) the Mer de Glace in 1823 (30.1 × 45.7 cm; pencil, pen, watercolor, bodycolor). Kupferstichkabinett, Kunstmuseum Basel. Photographs by Heinz J. Zumbühl.



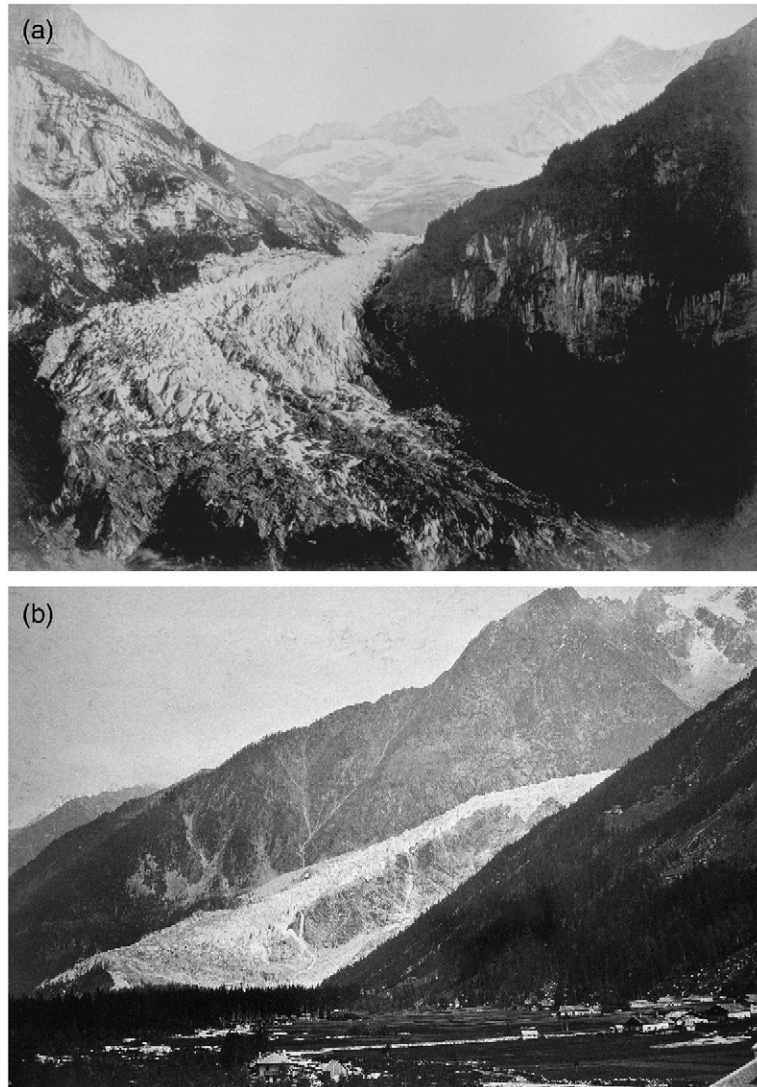


Fig. 5. Photographs from the Bisson Brothers showing (a) the Lower Grindelwald Glacier in 1855/56 (34.2 × 44.4 cm) and (b) the Mer de Glace in 1854 (34.1 × 45.4 cm). Alpine Club Library, London. Photographs by Heinz J. Zumbühl.

the growing interest for this subject during the last twenty years, we now have more possibilities to address this topic. For the probably oldest photograph of the Lower Grindelwald Glacier, there are three proofs: Firstly, the black ink stamp “Bisson frères” at the edge of the photo (this black stamp was only used from 1854–1857; see [Chlumsky et al., 1999](#)), secondly, travels to Switzerland in 1855/56 ([Chlumsky et al., 1999](#)), and thirdly, an advertisement of the Bisson Brothers in the journal “L’Artiste” (14 December 1856) give us strong evidence that the photograph was taken in 1855/56, during the mid 19th century maximum extension. Additionally, the photograph shows the glacier during late summer/early autumn season as there is a snow free

ice front. Starting from a high ice level just down in the valley (a big part of the “Schweif” existed) the front of the Lower Grindelwald Glacier advanced 75–150 m between 1839 (1843) and 1855/56 ([Zumbühl, 1980](#)).

In 1849, John Ruskin made the oldest photo known from the Mer de Glace in the area of Montanvers. Five years later, in 1854, the Bisson Brothers took a photo of the Glacier des Bois in the valley bottom, maybe the first one from this site ([de Decker Hefler, 2002](#); [Fig. 5b](#)). The frontal zone of the Mer de Glace advanced approximately 290 m from 1842 to 1852 ([Nussbaumer et al., in press](#)).

Comparable to previous views we can now look at the impressive glacier snouts in the valley bottom in

detail. In 1861, a partially collapsed snout of the Lower Grindelwald Glacier with the Lutschine (Fig. 6a) was photographed by Adolphe Braun (1812–1877; Kempf,

1994). In 1859, the archlike snout of the Mer de Glace with the source of the Arveyron river was still intact on the photo of the Bisson Brothers (Fig. 6b).

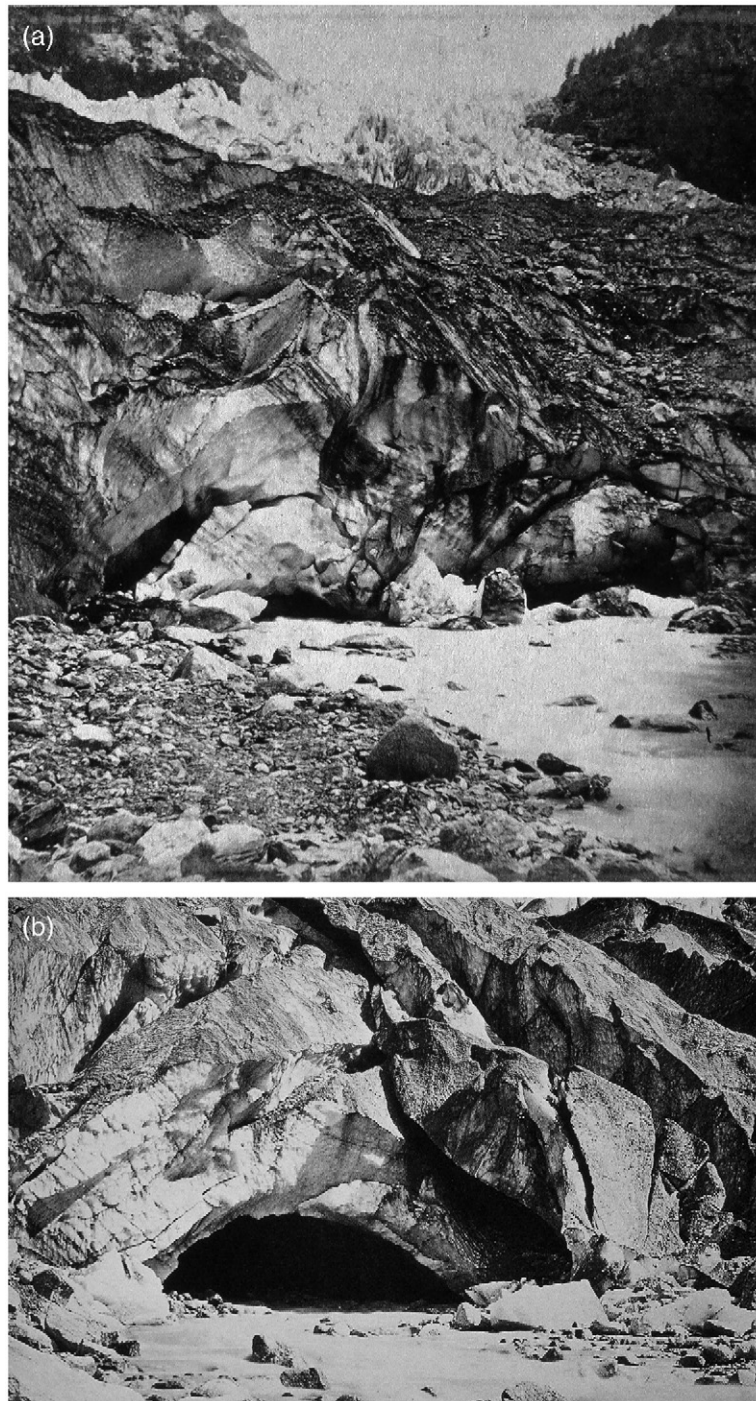


Fig. 6. (a) The snout of the Lower Grindelwald Glacier in 1861 (8.1 × 14.4 cm; cut-out). Stereograph “1109 Source de la Lutschine” by Adolphe Braun (1812–1877). Private Collection of Jaroslav F. Jebavy, Geneva. (b) The snout of the Mer de Glace in 1859 (23.2 × 39 cm). Photograph “Source de l’Arveyron” by the Bisson Brothers. Private collection of J. and S. Seydoux; Musée Savoisien, Chambéry (Exposition 2002).

### 3.3. The history of the two glaciers from the 19th century until today — Variations of length based on historical pictorial and written sources/documents

Historic length variation of the Lower Grindelwald Glacier (Fig. 7) belongs to the world's best-documented and longest ones of its kind thanks to a unique wealth of historic picture sources (Zumbühl, 1980; Zumbühl et al., 1983; Oerlemans, 2005). Since the 1980s we were able to collect new photographic documents which provide more detailed views of the mid 19th century ice margins (Steiner et al., *in press*).

The cumulative length curve of the Mer de Glace (Fig. 7) is the result of the studies of Mougin (1912) and Wetter (1987). Based on a huge collection of historical pictorial records, partly never studied before, Nussbaumer et al. (*in press*) refined the curve of length variations of the Mer de Glace.

Comparing the cumulative length curves of the Lower Grindelwald Glacier and the Mer de Glace for the 19th century yields the following results (Fig. 7): Both glaciers show a rapid advance at the beginning of the 19th century. The Lower Grindelwald Glacier reaches its first maximum extent in 1820/22, the Mer de Glace in 1821. In the following years both glaciers remain in or near the valley bottom, implying no significant retreat.

Then, in 1855/56 the Lower Grindelwald Glacier reached its second peak of the 19th century which was

bigger than the 1820/22 extent, while the Mer de Glace had the second peak of the 19th century in 1852/53 which was less pronounced than in 1821.

Finally, after the end of the LIA both glaciers retreated dramatically. The Lower Grindelwald Glacier melted back approximately 1000 m during the 1860–1880 period, the Mer de Glace showed a retreat of approximately 900 m during the 1867–1878 period.

### 3.4. Precipitation and temperature significance for the glacier variations in the 19th century

Here we explore the climatic forcings that may have been instrumental in the glacier fluctuations described above. Glacier mass balance and subsequent frontal response is influenced by climate, mainly temperature during the ablation season (summer) and precipitation during the accumulation season (winter). In an attempt to find consistency between glacier advances and both temperature and precipitation reconstructions, we compared the Lower Grindelwald Glacier (Switzerland) with precipitation reconstructions by Pauling et al. (2006) and temperature reconstructions by Luterbacher et al. (2004).

Before feeding the BPN, the input data was standardized to their mean and standard deviation over the whole training/verification period 1535–1983 so that temperature and precipitation are comparable (for a

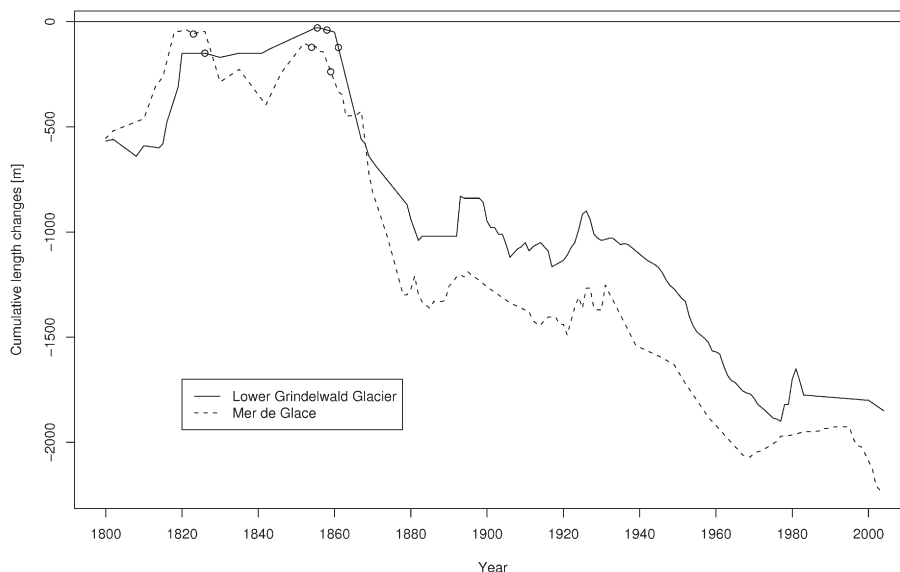


Fig. 7. Cumulative length variations of the Lower Grindelwald Glacier (solid line; Zumbühl, 1980; Holzhauser and Zumbühl, 1996, 2003; Steiner et al., *in press*) and the Mer de Glace (dashed line; data 1911–2003 from the Laboratoire de Glaciologie et Géophysique de l'Environnement LGGE; Nussbaumer et al., *in press*) from 1800 onwards, relative to the 1600s maximum extent. The points on the curves indicate the ice margin locations as depicted in Figs. 3–6 and 9–10.



robust NN performance). As explained before, each climate input has been stepwise shifted in time so that all lags between 0 and 45 years have been used. This was done to account for the varying reaction time of the glacier. The lag time has been fixed according to [Schmeits and Oerlemans \(1997\)](#), and [Haerberli and Hoelzle \(1995\)](#), respectively, which calculated a response time for the Lower Grindelwald Glacier of 34–45 years, and 20–30 years, respectively. Furthermore, it must be noted that the reaction to climate at the glacier snout can also be more immediate in some situations, e.g. after runs of cool summers ([Matthews and Briffa, 2005](#)).

To investigate the relative importance of the influential factors we performed a sensitivity analysis using neural networks based on winter (Prec\_DJF), spring (Prec\_MAM) and autumn precipitation (Prec\_SON) as well as spring (Temp\_MAM: [Xoplaki et al., 2005](#)), summer (Temp\_JJA) and autumn temperature (Temp\_SON: [Xoplaki et al., 2005](#)) as input variables of the Backpropagation Neural Network (BPN) ([Fig. 2](#)). An analysis of the Seasonal Sensitivity Characteristics (SSCs) of the Lower Grindelwald Glacier showed that summer (JJA) precipitation and winter (DJF) temperature do not lead to a strong response in mass balance and

therefore glacier length. So, these two time series are not used as input variables ([Oerlemans and Reichert, 2000](#); [Reichert et al., 2001](#); personal communication by Johannes Oerlemans, University of Utrecht, 10.8.2005).

After training the BPN, one input has been set to its mean and the rest of the inputs to their real values. The trained model has been fed with this new pattern. By comparing the network error of the original model with the error resulting from the new pattern, we can establish a relative importance of the changed input variable. This procedure is repeated for each input variable.

[Fig. 8](#) shows a boxplot describing the relative importance of the input data for the 1810–1820 advance and 1860–1880 retreat period of the Lower Grindelwald Glacier ([Zumbühl, 1980](#); [Zumbühl et al., 1983](#); [Holzhauser and Zumbühl, 2003](#)). Each boxplot is based on the average outputs of 30 model runs with different lags as input to reduce the effect of falling into local minima ([Steiner et al., 2005](#)). This resulted in an assessment of the relative importance of the input variables.

The 1810–1820 advance ([Fig. 8a](#)), which marks the beginning of the mid 19th century maximum glacier extent, was presumably driven by low summer tempera-

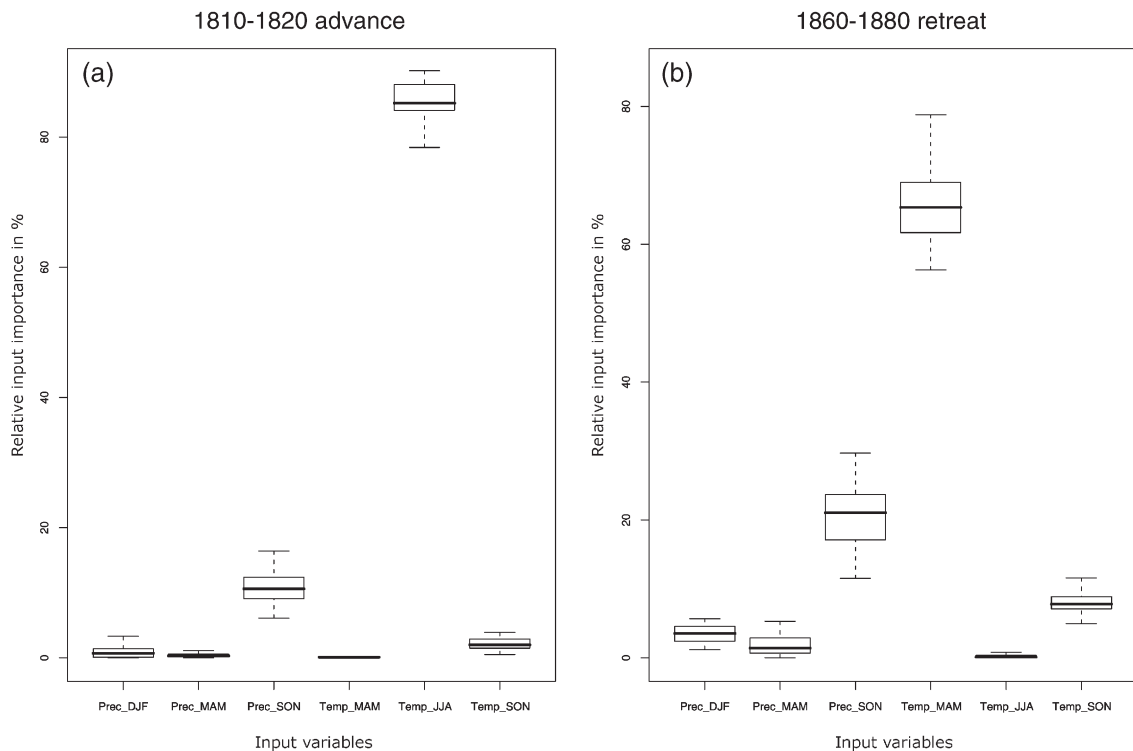


**Fig. 8.** Relative importance of climate input variables to length fluctuations of the Lower Grindelwald Glacier (Switzerland) for the following periods: (a) 1810–1820 advance period, (b) 1860–1880 retreat period. For each input variable to the neural network the median, the first and third quartile (lower/upper hinge) and a 95% confidence interval for the median (lower/upper whisker) of the 30 model runs are given.



tures (more than 80% relative input importance) and high autumn precipitation. Note that in this case the variability of the relative importance is lower compared to other advance periods (not shown). Furthermore, this advance shows specifically the expected pattern of an advancing Alpine glacier: Low summer temperatures during the advance period hinder ablation making glacier advances possible. Above normal (autumn) precipitation leads to a positive mass balance in the accumulation area. This is a prerequisite for later advances of the glacier snout.

It is not surprising that the 1860–1880 retreat period was mainly driven by high temperatures. High spring temperatures and decreasing autumn precipitation could have been the cause for the 1860–1880 retreat (Fig. 8b).

#### 4. Discussion and conclusions

The Lower Grindelwald Glacier and the Mer de Glace are among the best-documented glaciers with different kinds of historical sources. The high-quality drawings by Samuel Birman and the first photo-

graphs by the Bisson Brothers and others are both outstanding examples of glacier representations from the last part of the Little Ice Age (LIA). Pictorial sources therefore provide insight into glacier changes as well as on changing views on glaciers. As a consequence, we are able to do both comparisons of glacier representations and a qualitative analysis of glacier variations. Figs. 9 and 10 show the enormous glacier changes that have occurred since the last LIA glacier maximum extent.

After analyzing new documentary data, we show that the series of length fluctuations of the Lower Grindelwald Glacier and the revised curve of the length fluctuations of the Mer de Glace are very similar – despite the big spatial distance between the glaciers.

The analysis of historical sources and the hereby derived quantitative data are the prerequisite to study the connection between climatic driving factors and glacier changes. In a new nonlinear neural network approach which has been successfully applied to analyze the sensitivity of the Lower Grindelwald Glacier to different climate parameters, we show that

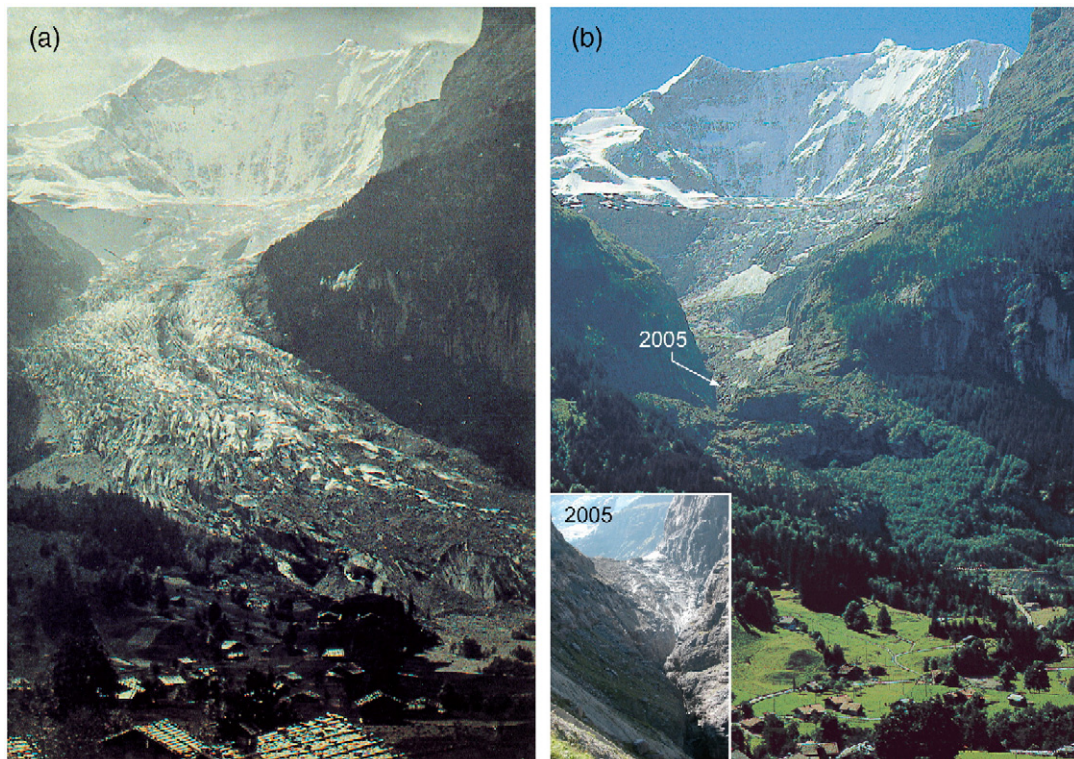


Fig. 9. (a) The Lower Grindelwald Glacier 1858 in the valley floor, 2–3 years after the maximum extent in 1855/56 ( $31.9 \times 25.2$  km). Photograph by Frédéric Martens (1806–1885). Alpine Club Library, London. Photograph by Heinz J. Zumbühl. (b) The Lower Grindelwald Glacier 1974. Photograph by Heinz J. Zumbühl, 23.7.1974. Also given is a recent view of the glacier gorge. Photograph by Andreas Bauder, 7.9.2005. The arrow shows the location of the glacier front in 2005.

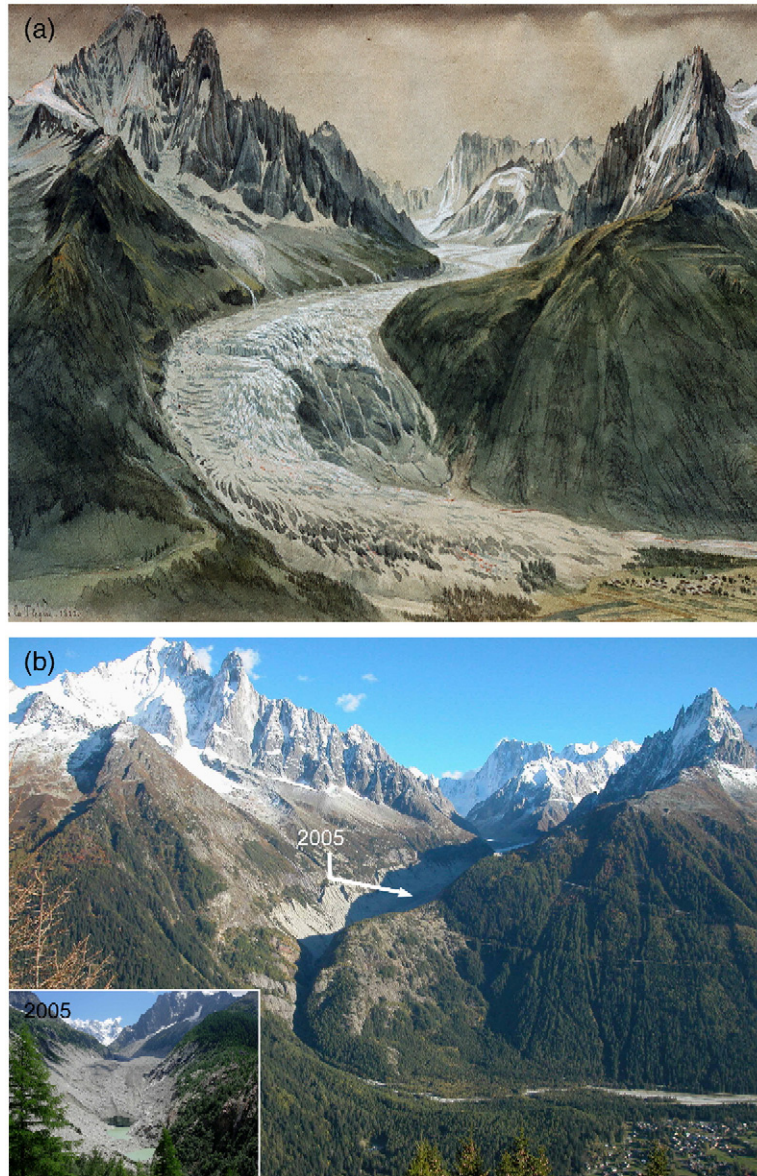


Fig. 10. (a) Samuel Birmann portrayed in 1823 the Mer de Glace 1823 from la Flégère (20.6 × 47.1 cm; pencil, pen, watercolor, bodycolor; cut-out). Kupferstichkabinett, Kunstmuseum Basel. Photograph by Heinz J. Zumbühl. (b) Recent view of the Mer de Glace. Photograph by Samuel U. Nussbaumer, 8.10.2005. Again, the arrow shows the location of the glacier front in 2005.

different configurations of climate variables lead to a glacier advance/retreat. The advance towards 1820 was presumably driven by low summer temperatures and high autumn precipitation. The 1860–1880 retreat period was mainly determined by high temperatures. However, temperature seems to be the primary driver of the mid 19th maximum extent and subsequent retreat, precipitation plays a secondary role. We also conclude that the Lower Grindelwald Glacier shows a time-dependent, dynamic response to climatic change.

Length variations are shown to behave as a lagged process, with a glacier-specific memory of past climatic conditions.

Finally, the present nonlinear neural network approach seems to be a powerful tool in a glaciological context. Because the limitations and chances of this nonlinear technique are not fully explored, further investigations towards a “neuro-glaciology” should be done, including different glaciers in different climate regions.



## Acknowledgements

This study was supported by the Swiss National Science Foundation, through its National Centre of Competence in Research on Climate (NCCR Climate), project PALVAREX. The authors are grateful to J. Luterbacher and A. Pauling for providing multiproxy reconstructions of temperature and precipitation. Thanks also go to C. Vincent and the LGGE (Laboratoire de Glaciologie et Géophysique de l'Environnement, Saint-Martin-d'Hères cedex, France) for providing data from the Mer de Glace. We also wish to thank R. Eggimann and D. Mihajlovic from Photogrammetrie Perrinjaquet AG, Gümligen, Switzerland, for their help in photogrammetric interpretation of aerial photographs and the generation of digital elevation models (DEMs).

## References

- Birmann, S., 1826. *Souvenirs de la Vallée de Chamonix*. Birmann et fils, Basel.
- Chlumsky, M., Eskildsen, U., Marbot, B., 1999. Die Brüder Bisson. Aufstieg und Fall eines Fotografenunternehmens im 19. Jahrhundert. Katalog zur gleichnamigen Ausstellung: Museum Folkwang, Essen, 07.02.–28.03.1999; Fotomuseum im Münchner Stadtmuseum, 11.04.–30.05.1999; Bibliothèque nationale de France, Paris, 15.06.–15.08.1999. Verlag der Kunst, Amsterdam.
- de Decker Heflter, S., 2002. *Photographier le Mont Blanc. Les pionniers* – Collection Sophie et Jérôme Seydoux. Editions Guérin, Chamonix.
- Grove, J.M., 2004. *Little Ice Ages: Ancient and Modern*, 2nd edition. Routledge, London.
- Haerberli, W., Hoelzle, M., 1995. Application of inventory data for estimating characteristics of and regional climate-change effects on mountain glaciers: a pilot study with the European Alps. *Annals of Glaciology* 21, 206–212.
- Haerberli, W., Zumbühl, H.J., 2003. Schwankungen der Alpengletscher im Wandel von Klima und Perzeption. In: Jeanneret, F., Wastl-Walter, D., Wiesmann, U., Schwyn, M. (Eds.), *Welt der Alpen – Gebirge der Welt, Ressourcen, Akteure, Perspektiven*. Haupt, Bern, pp. 77–92.
- Holzhauser, H., Zumbühl, H.J., 1996. To the history of the Lower Grindelwald Glacier during the last 2800 years – palaeosols, fossil wood and historical pictorial records – new results. *Zeitschrift für Geomorphologie, Neue Folge, Supplementband* 104, 95–127.
- Holzhauser, H., Zumbühl, H.J., 2003. Nacheiszeitliche Gletscherschwankungen. In: Weingartner, R., Spreafico, M. (Eds.), *Hydrologischer Atlas der Schweiz. Special edition for the 54th “Deutscher Geographentag” in Berne (revised)*. Bundesamt für Landestopografie, Bern-Wabern.
- Holzhauser, H., Magny, M., Zumbühl, H.J., 2005. Glacier and lake-level variations in west-central Europe over the last 3500 years. *The Holocene* 15 (6), 791–803.
- Imhof, M., 1998. Rock glaciers, Bernese Alps, western Switzerland. In: *International Permafrost Association, Data and Information Working Group (Eds.), National Snow and Ice Data Center (NSIDC)/World Data Center for Glaciology, University of Colorado, Boulder, CO, CD-ROM*.
- Kempf, C., 1994. Adolphe Braun et la photographie, 1812–1877. Editions Lucigraphie/Valblor, Illkirch, France.
- Kirchhofer, W., Sevruk, B., 1992. Mittlere jährliche korrigierte Niederschlagshöhen 1951–1980. In: Weingartner, R., Spreafico, M. (Eds.), *Hydrologischer Atlas der Schweiz. Bundesamt für Landestopografie, Bern-Wabern*.
- Luterbacher, J., Dietrich, D., Xoplaki, E., Grosjean, M., Wanner, H., 2004. European seasonal and annual temperature variability, trends, and extremes since 1500. *Science* 303 (5663), 1499–1503.
- Maisch, M., Wipf, A., Denmeler, B., Battaglia, J., Benz, C., 1999. Die Gletscher der Schweizer Alpen. Gletscherhochstand 1850, Aktuelle Vergletscherung, Gletscherschwund-Szenarien. Vdf Hochschulverlag, ETH Zürich.
- Matthews, J.A., Briffa, K.R., 2005. The ‘Little Ice Age’: re-evaluation of an evolving concept. *Geografiska Annaler* 87A (1), 17–36.
- Michaelsen, J., 1987. Cross-validation in statistical climate forecast models. *Journal of Applied Meteorology* 26 (11), 1589–1600.
- Mougin, P., 1912. *Etudes glaciologiques. Savoie-Pyrénées, Tome III*. Imprimerie Nationale, Paris.
- Nussbaumer, S.U., Zumbühl, H.J., Steiner, D., in press. Fluctuations of the “Mer de Glace” (Mont Blanc area, France) AD 1500–2050: an interdisciplinary approach using new historical data and neural network simulations. *Zeitschrift für Gletscherkunde und Glazialgeologie*.
- Oerlemans, J., 2005. Extracting a climate signal from 169 glacier records. *Science* 308 (5722), 675–677.
- Oerlemans, J., Reichert, B.K., 2000. Relating glacier mass balance to meteorological data by using a seasonal sensitivity characteristic. *Journal of Glaciology* 46 (152), 1–6.
- Pauling, A., Luterbacher, J., Casty, C., Wanner, H., 2006. Five hundred years of gridded high-resolution precipitation reconstructions over Europe and the connection to large-scale circulation. *Climate Dynamics* 26 (4), 387–405.
- Reichert, B.K., Bengtsson, L., Oerlemans, J., 2001. Midlatitude forcing mechanisms for glacier mass balance investigated using general circulation models. *Journal of Climate* 14 (17), 3767–3784.
- Rumelhart, D.E., Hinton, G.E., Williams, R.J., 1986. Learning internal representations by error propagation. In: Rumelhart, D.E., McClelland, J.L. (Eds.), *Parallel Distributed Processing: Explorations in the Microstructure of Cognition*. MIT Press, Cambridge, MA, pp. 318–362.
- Schmeits, M.J., Oerlemans, J., 1997. Simulation of the historical variations in length of Unterer Grindelwaldgletscher, Switzerland. *Journal of Glaciology* 43 (143), 152–164.
- Steiner, D., Walter, A., Zumbühl, H.J., 2005. The application of a non-linear back-propagation neural network to study the mass balance of Grosse Aletschgletscher, Switzerland. *Journal of Glaciology* 51 (173), 313–323.
- Steiner, D., Zumbühl, H.J., Bauder, A., in press. Two Alpine Glaciers over the Past Two Centuries: A Scientific View Based on Pictorial Sources. In: Orlove, B., Wiegandt, E., Luckman, B. (Eds.), *Darkening Peaks: Glacial Retreat, Science and Society*. University of California Press, Berkeley, CA.
- Stone, M., 1974. Cross-validation choice and the assessment of statistical predictions. *Journal of the Royal Statistical Society. Series B* 36 (1), 111–147.
- Walter, A., Schönwiese, C.-D., 2002. Attribution and detection of anthropogenic climate change using a backpropagation neural network. *Meteorologische Zeitschrift* 11 (5), 335–343.

- Walter, A., Schönwiese, C.-D., 2003. Nonlinear statistical attribution and detection of anthropogenic climate change using simulated annealing algorithm. *Theoretical and Applied Climatology* 76 (1–2), 1–12.
- Wang, W., Jones, P., Partridge, D., 2000. Assessing the impact of input features in a feedforward neural network. *Neural Computing and Applications* 9 (2), 101–112.
- Wetter, W., 1987. Spät- und postglaziale Gletscherschwankungen im Mont Blanc-Gebiet: Untere Vallée de Chamonix – Val Montjoie. *Physische Geographie*, Vol. 22. Geographisches Institut der Universität Zürich, Zürich.
- Xoplaki, E., Luterbacher, J., Paeth, H., Dietrich, D., Steiner, N., Grosjean, M., Wanner, H., 2005. European spring and autumn temperature variability and change of extremes over the last half millennium. *Geophysical Research Letters* 32 (15), L15713.
- Zumbühl, H.J., 1980. Die Schwankungen der Grindelwaldgletscher in den historischen Bild- und Schriftquellen des 12. bis 19. Jahrhunderts. Ein Beitrag zur Gletschergeschichte und Erforschung des Alpenraumes. *Denkschriften der Schweizerischen Naturforschenden Gesellschaft (SNG)*, Band 92. Birkhäuser, Basel/Boston/Stuttgart.
- Zumbühl, H.J., 1997. Die Hochgebirgszeichnungen von Samuel Birmann – ihre Bedeutung für die Gletscher- und Klimageschichte. Katalog zur Ausstellung “Peter und Samuel Birmann – Künstler, Sammler, Händler, Stifter” des Kunstmuseums Basel vom 27.09.1997–11.01.1998. Schwabe Verlag, Basel.
- Zumbühl, H.J., Holzhauser, H., 1988. Alpengletscher in der Kleinen Eiszeit. Sonderheft zum 125jährigen Jubiläum des SAC. *Die Alpen* 64 (3), 129–322.
- Zumbühl, H.J., Messerli, B., Pfister, C., 1983. Die kleine Eiszeit: Gletschergeschichte im Spiegel der Kunst. Katalog zur Sonderausstellung des Schweizerischen Alpen Museums Bern und des Gletschergarten-Museums Luzern vom 09.06.–14.08.1983 (Luzern), 24.08.–16.10.1983 (Bern).